

ZULFAQAR Journal of Defence Science, Engineering & Technology

e-ISSN: 2773-5281 Vol. 8, Issue 2 (2025)

DOI: https://doi.org/10.58247/jdset-2025-0802-20

Journal homepage: https://zulfaqarjdset.upnm.edu.my



LITERATURE STUDY ON DESIGNING CONTROL LAW FOR CONVENTIONAL FIXED-WING UAV USING CONVENTIONAL AIRCRAFT CONTROL LAW APPROACH

Zuhairi Abdul Rashida, b*, Syed Mohd Fairuz Syed Mohd Dardina, Khairol Amali Ahmada

- ^a Department of Electrical & Electronic, Faculty of Engineering, National Defence University of Malaysia, Sg. Besi Camp, 57000 Kuala Lumpur, Malaysia
- ^b Army Logistic Command Headquarters, Electrical & Mechanical Engineering Group, Imphal Camp, Jalan Padang Tembak, 50634 Kuala Lumpur, Malaysia

ARTICLE INFO

ARTICLE HISTORY

Received: 01-04-2025 Revised: 10-06-2025 Accepted: 01-07-2025 Published: 30-11-2025

KEYWORDS

UAV Aircraft Natural characteristic System modelling

ABSTRACT

The significant differences between conventional fixed wing aircraft system and a fixed wing Unmanned Aerial Vehicle (UAV) system are the sized and the number of sensors onboard each system. With this constraint, smaller UAV will have a simpler control law design compared to the complex control law of a conventional aircraft. This literature review is studied on the comparison between the available conventional aircraft with the current developed UAV in terms of their inputs, outputs, modelling method, flight modes, and control law design. Finding on the literature shows that it is possible to design a control law for UAV similar to conventional aircraft control law using current technology (sensor and microcontroller). However, there are critical requirement for the drift angle measurement module which needed to be developed first before the modelling and control law can be designed.

1.0 INTRODUCTION

There are significant differences between conventional fixed wing aircraft and Unmanned Aerial Vehicle (UAV). The biggest difference would be the larger sized of conventional aircraft compare to smaller sizes of an UAVs. With the larger size, the conventional aircraft would be able to be equipped with larger number of sensors as well as better sensors which usually come in larger sizes. However, as technology progresses, sensor are becoming much smaller with decent performance in sensing capabilities. This is true especially for Micro-electromechanical Systems or MEMS sensor which can incorporate between optical, mechanical, and electronics part into a single microchip [1]. The design of complex control laws for conventional aircraft is possible due to complex system of sensors integration and substantial computational power of the onboard computer to calculate and correcting the aircraft attitude during flight. If the same attitude control laws can be implemented onto a UAVs, the UAV may be able to perform better in harsh condition such as heavy crosswind condition. However, the same state or outputs that can be measured by the UAV must be equal to one that conventional aircraft can measured.

The literature study will be done by comparing the similarity and possibility of method used for controlling attitude between conventional fixed-wing aircraft with the fixed-wing UAV. This will allow for the greater outcome of evaluating the possibility for UAV to have the same attitude control laws as the conventional aircraft have. The literature study will include the inputs and outputs for each system, the sensors use for conventional aircraft and UAVs, the modelling of conventional aircraft and UAVs, the flight modes for conventional aircraft and UAVs, the controller design method uses for conventional aircraft and UAVs and the comparison between conventional aircraft and UAVs. The conventional aircraft that will be studied for this project will be the Airbus A320 (later will be known as the conventional aircraft) which is a fixed wing type aircraft with twin turbine engine configuration. Several known UAVs will be studied and compared in this paper which has been developed by other researchers with similar objective of designing

control laws for their specific UAV. The UAV studied for this paper are listed as the P15035 Aircraft, the PEGASE delta wing mini-UAV and the BPPT Wulung UAV.

2.0 THE CONVENTIONAL AIRCRAFT SYSTEM

The conventional aircraft studied for this project is the Airbus A320 aircraft. This aircraft is a fixed wing type aircraft with a twin turbine engine configuration. The Airbus A320 aircraft is as shown in Figure 1. The basic configuration of a conventional fixed wing aircraft such as in Figure 1 is for it to have a basic control surface configuration and twin-engine configurations.



Figure 1. The Airbus A320 Aircraft [2]

2.1 The Inputs for Conventional Aircraft System

The input for controlling the conventional aircraft will be the control column, and paddles. These are known as pilot control input. The pilot control input will be used to control the movement of the control surfaces. The basic control surfaces for Airbus A320 aircraft are the ailerons, the rudder, the elevator and trimmable horizontal tailplane [3]. The control surfaces are used to control the aircraft attitude which are the movement of rotation along the aircraft centre of gravity (CoG). The aircraft attitude is represented as in Figure 2. The attitude movement in Figure 2 is also applied for UAV. The relation from the pilot control input for the aircraft attitude is represented as in Table 1.

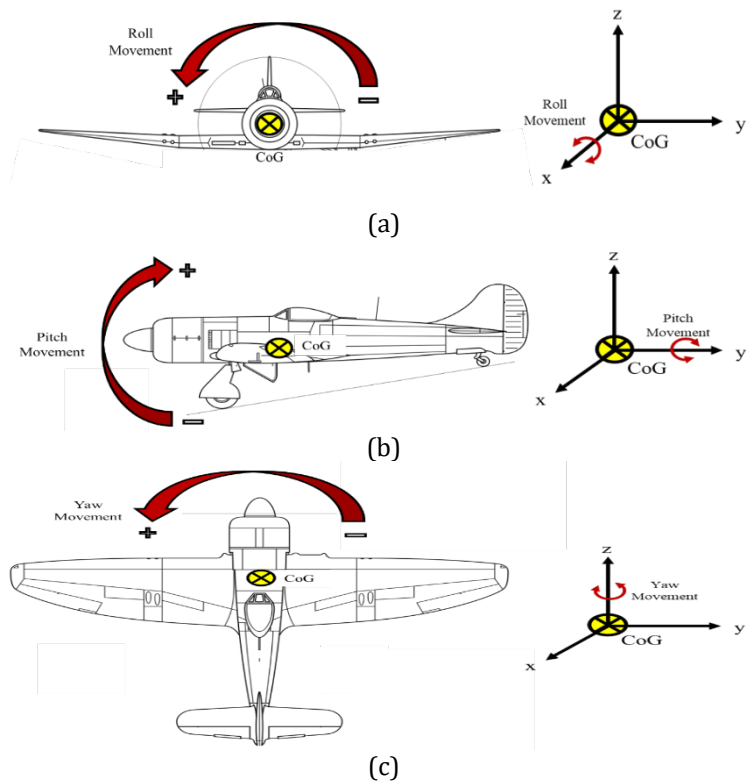


Figure 2. Attitude movement for conventional fixed wing aircraft, (a) Roll movement – rotation on x-axis., (b) Pitch movement – rotation on y-axis., (c) Yaw movement – rotation on z-axis

The control surfaces and aircraft attitude represented in Table 1 is a basic notation on how an aircraft control work. The flight characteristics of an aircraft, however, are determined between the control surfaces with the attitude movement of the aircraft. Thus, for modelling the flight characteristic of a

conventional aircraft, the input will be the control surfaces, and the outputs will be the attitude movement. The input for conventional aircraft will be the control surfaces tabulated as in Table 2.

Table 1. The relation from the pilot control input util the attitude movement

Pilot Control Inputs	Control Surfaces	Attitude
Control Stick	Ailerons	Roll
Control Stick	Elevator	Pitch
Paddles	Rudder	Yaw
Pitch Trim	Trimmable Horizontal Tailplane	Pitch

Table 2. Inputs for conventional aircraft and symbols

Table 2: inputs for conventional an erart and symbols		
Inputs	Symbol	Remarks
Ailerons Deflection (rad)	δa	Lateral Motion
Rudder Deflection (rad)	δr	Lateral Motion
Elevator Deflection (rad)	δe	Longitudinal Motion
Pitch Trim Deflection (rad)	δm	Longitudinal Motion

2.2 The Outputs for Conventional Aircraft System

It was established previously that the inputs for modelling the flight characteristic of a conventional will be the control surfaces of the aircraft while the outputs will be the attitude movement or rotations around the CoG. However, for conventional aircraft, the attitude measurement is not enough to control the aircraft for during flight. The drift angles need to be measured and feedback with the inputs are required in ensuring the aircraft flown safely avoiding wind gust. The outputs for conventional aircraft modelling now consist of attitude movement and drift angle measurement. For these outputs to be useful, they need to be measurable and controllable. The measurement for attitude movement and drift angle is done using the sensor in Table 3. Table 3 shows multiple measurement can be obtained from several sensors onboard the conventional aircraft. However, only eight outputs that been calculated from the fusion of data from the Table 3 will be used for modelling the conventional aircraft are as shown in Table 4.

Table 3. Sensor onboard conventional aircraft and their usage [3]

Sensor	Measurement	Notation	Unit	Usage
	Static Pressure Total Pressure	P_s	mbar mbar	Airspeed
Air Data Reference	Total Air Temperature	P _T TAT	°C	computation
	Angle of Attack	α	deg	α calculation
	Side Slip Angle	β	deg	β calculation
	Acceleration	N_x , N_y , N_z	g	Lateral and
Inertial Reference	Angular Rate	p, q, r	deg/s	longitudinal
	Attitudes	θ, φ, ψ	deg	control law
System (IRS)	Ground Speed	V_{gnd}	kts	Speed control
	Track Angle	TRK	deg	Track control

Table 4. Outputs or measurement calculated for conventional aircraft modelling

State or Output	Symbol	Remarks
Side Slip Angle (rad)	β	Lateral Motion
Yaw Rate (rad/s)	r	Lateral Motion
Roll Rate (rad/s)	p	Lateral Motion
Bank Angle (rad)	Ø	Lateral Motion
Airspeed (m/s)	V	Longitudinal Motion
Flight Path Angle	γ	Longitudinal Motion
Angle of Attack (rad)	α	Longitudinal Motion
Pitch Rate (rad/s)	q	Longitudinal Motion

The sensors list in Table 3 with measurements in Table 4 are not singular but rather multiple in numbers. The sensors are also located in multiple places on the aircraft for better reading, redundancy, and segregation purposes. The outputs or measurement calculated in Table 4 is using multiple flight computer

which constantly calculated and interpreting raw values from the sensors to become a useful data. Examples of locations of sensors onboard a conventional aircraft are as shown in Figure 3.

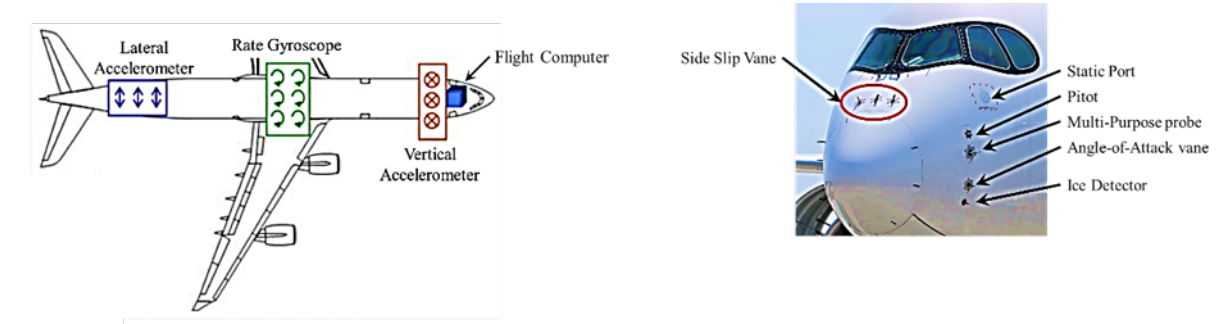


Figure 3. Sensor's location onboard a conventional aircraft [4]

In Figure 3, the Air Data Reference sensors are mostly located on the nosecone of the conventional aircraft while the IRS sensors are located across the whole fuselage of the conventional aircraft. The mathematical modelling of the natural flight characteristics for a conventional aircraft will be based on the defined inputs and outputs mentioned in Table 1 and Table 4.

2.3 The Modelling for Conventional Aircraft System

The modelling for conventional aircraft is a complex process involving the computational modelling and simulations, wind tunnel testing, and flight testing to ensure that the modelling is correctly represented the actual flight characteristic of conventional aircraft. Normally, the modelling of an aircraft is represented in form of state-space representation which mathematically represented as in (1). This is due to the nature of the state-space modelling which enables the system that has been represented to be a Multiple-Inputs Multiple-Outputs (MIMO) system.

$$\dot{X} = A \cdot X + B \cdot U$$

$$Y = C \cdot X$$
(1)

where

X is the state vector, U is the output vector, Y is the output vector, A is the state matrix, B is the input matrix, and C is the output matrix. The modelling for conventional aircraft is done by assuming that lateral motions are independent from longitudinal motions. This led to two state representation for lateral flight and for longitudinal flight. The modelling for lateral flight is as shown in (2) and modelling for longitudinal flight is as shown as in (3).

For lateral modelling in (2), the state matrix composes of sideslip angle, yaw rate, roll rate, and bank angle which represented by β , r, p, and \emptyset respectively. The state-space also contain variables for airspeed and angle-of-attack which represented by V and α respectively. The inputs for the state-space are the ailerons deflection angle and rudder deflection angle which represented by δ_a and δ_r respectively. The Y_β , $Y_{\delta a}$, $Y_{\delta r}$, N_β , N_r , N_β , $N_{\delta r}$, L_β , L_r , L_β , L_r , L_δ , and $L_{\delta r}$ represent the lateral-directional derivatives which their values obtained through wind tunnel testing and simulations of the aircraft. For longitudinal modelling in (3), the state matrix composes of airspeed, flight path, angle-of-attack and pitch rate which represented by V_γ , V_γ ,

$$\begin{pmatrix}
\dot{\beta} \\
\dot{r} \\
\dot{p} \\
\dot{\phi}
\end{pmatrix} = \begin{pmatrix}
\frac{Y_{\beta}}{V} & -\cos\alpha & \sin\alpha & \frac{g \cdot \cos\theta}{V} \\
N_{\beta} & N_{r} & N_{p} & 0 \\
L_{\beta} & L_{r} & L_{p} & 0 \\
0 & \tan\theta & 1 & 0
\end{pmatrix} \cdot \begin{pmatrix}
\beta \\
r \\
p \\
\phi
\end{pmatrix} + \begin{pmatrix}
\frac{Y_{\delta a}}{V} & \frac{Y_{\delta r}}{V} \\
N_{\delta a} & N_{\delta r} \\
L_{\delta a} & L_{\delta r} \\
0 & 0
\end{pmatrix} \cdot \begin{pmatrix}
\delta a \\
\delta r
\end{pmatrix}$$

$$Y = \begin{pmatrix}
1 & 0 & 0 & 0 \\
0 & 1 & 0 & 0 \\
0 & 0 & 1 & 0 \\
0 & 0 & 0 & 1
\end{pmatrix} \cdot \begin{pmatrix}
\beta \\
r \\
p \\
\phi
\end{pmatrix}$$

$$\begin{pmatrix}
\dot{V} \\
\dot{\gamma} \\
\dot{\alpha} \\
\dot{q}
\end{pmatrix} = \begin{pmatrix}
x_{V} & x_{Y} & x_{\alpha} & x_{q} \\
z_{V} & 0 & z_{\alpha} & z_{q} \\
-z_{V} & 0 & -z_{\alpha} & (1-z_{q}) \\
0 & 0 & m_{\alpha} & m_{q}
\end{pmatrix} \cdot \begin{pmatrix}
V \\
\gamma \\
\alpha \\
q
\end{pmatrix} + \begin{pmatrix}
x_{\delta e} & x_{\delta m} \\
0 & z_{\delta m} \\
0 & -z_{\delta m} \\
0 & m_{\delta m}
\end{pmatrix} \cdot \begin{pmatrix}\delta e \\
\delta m
\end{pmatrix}$$
(3)

$$Y = \begin{pmatrix} 1 & 0 & 0 & 0 \\ 0 & 1 & 0 & 0 \\ 0 & 0 & 1 & 0 \\ 0 & 0 & 0 & 1 \end{pmatrix} \cdot \begin{pmatrix} V \\ \gamma \\ \alpha \\ q \end{pmatrix}$$
(3)

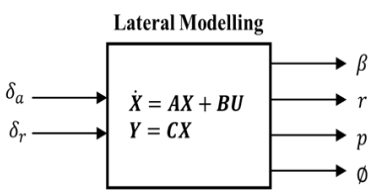


Figure 4. Lateral modelling block diagram for conventional aircraft

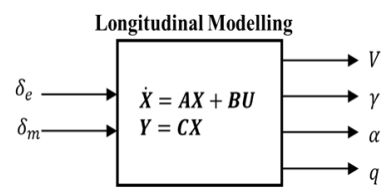


Figure 5. Longitudinal modelling block diagram for conventional aircraft

In Figure 4, the inputs for lateral modelling will be the ailerons deflections and rudder deflection with the modelling outputs of the side-slip angle, yaw rate, roll rate, and bank angle. In Figure 5, the inputs for longitudinal modelling will be the elevator deflection and the pitch trim deflection for the trimmable horizontal tailplane with the modelling outputs of airspeed, flight path angle, angle-of-attack, and pitch rate. In (2) and (3) the outputs and states of the lateral and longitudinal modelling for conventional aircraft are the same. This is designed for easy calculation and design for the feedback system. The outputs or states for the aircraft modelling are the same as the identified outputs stated in Table 4. The inputs for the modelling are the control surfaces deflections instead of the pilot control inputs. This is because between the pilot control input and the control surfaces, there will be a transient response which affects the mathematical modelling processes. The input for conventional aircraft modelling remains as in Table 2. The parameters in the state matrix and input matrix are obtained through computational analysis and wind tunnel testing. These parameters are called the Lateral Directional Derivative and the Longitudinal Directional Derivative. This thesis will not derive the process obtaining the two directional derivatives due to the complexity of calculation and they are not relevant to the overall project.

2.4 The Conventional Aircraft Flight Modes

The flight modes for conventional aircraft determines how the aircraft behave during flight. There are five flight modes for conventional aircraft where three of them is for lateral flight and two for longitudinal flight. The detail explanation for each mode is as follows:

Roll Mode

This is the fastest mode in lateral flight characteristics. This mode represents how fast the aircraft will roll when ailerons been deflected. The response time for this mode is between 0.4s to 5s which indicate that the aircraft will tent to roll immediately after the ailerons deflected. This mode is illustrated as in Figure 6.

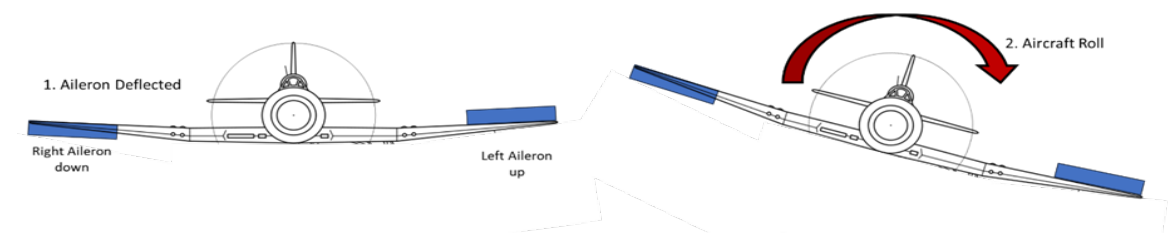


Figure 4. Roll Mode for conventional aircraft

Spiral Mode

This mode represents how the aircraft spiral during coordinated turn. This is the slowest mode in lateral flight characteristics. This mode relates between roll induced yaw (Figure 7) and yaw induced roll (Figure 8). If the effect of roll induced yaw is greater than the effect of yaw induced roll, then the aircraft will have a low spiral stability but better manoeuvrability. Vice versa, when the effect of yaw induced roll is greater, then the aircraft will tend to have a higher spiral stability with worsen manoeuvrability. The spiral stability is illustrated as in Figure 9.

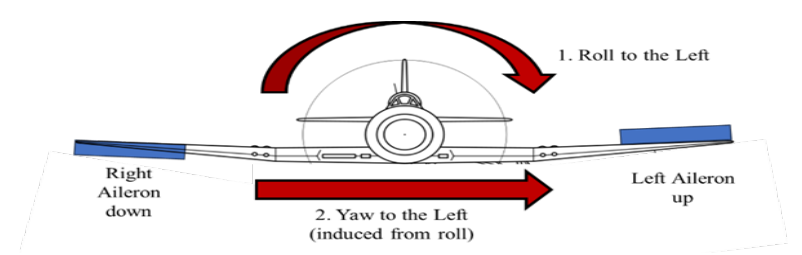


Figure 7. Roll induced Yaw. When the aircraft is rolling, the aircraft will tend to yaw

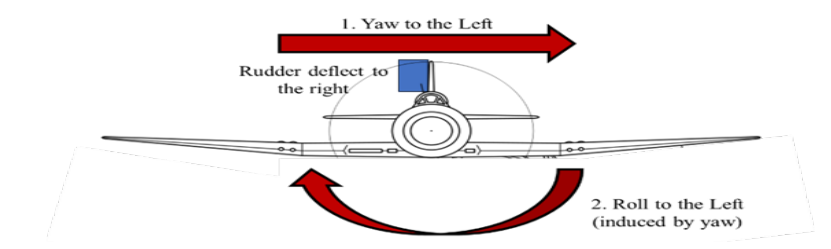


Figure 5. Yaw induced Roll. When the aircraft is yawing, the aircraft will tend to roll

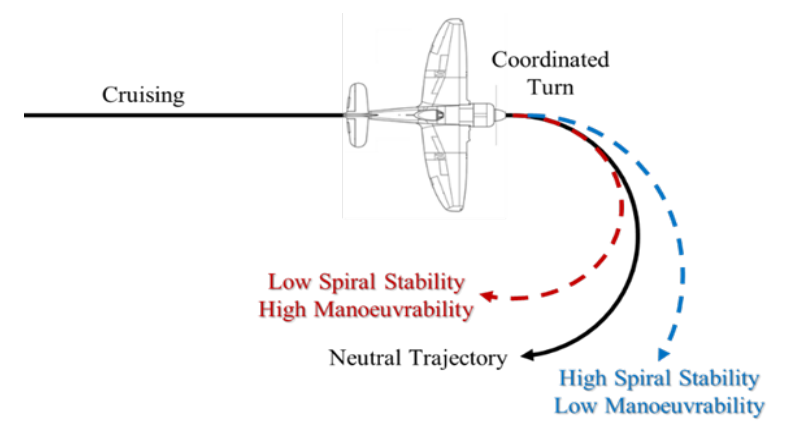


Figure 6. Spiral Mode for conventional aircraft. The balance between spiral stability and manoeuvrability are required during flight

Dutch Roll Mode

This is the only oscillation mode for lateral flight characteristics. This mode represents the oscillation occur between the sideslip and bank angle in opposite directions of the aircraft during flight. Simpler way to visualise this mode is by seeing the wing tip of the aircraft making an elliptical shape during flight. This mode is illustrated as in Figure 10.

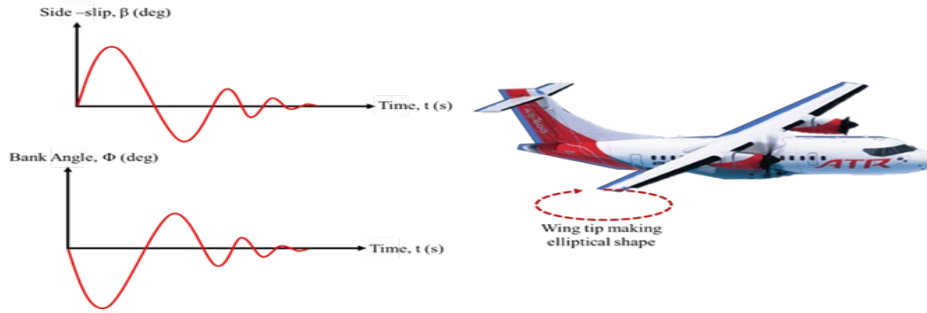


Figure 7. Dutch Roll Mode for conventional aircraft. Oscillation occurs between side-slip angle and bank angle forcing the wing tips to create an elliptical motion during flight

Short Period Mode

This mode is one of the two longitudinal modes for conventional flight characteristic. This mode represents the oscillation of angle of attack along the centre of gravity of an aircraft. The transient response of this mode occurs between 0.4s to 5s. The illustration for this mode is as in Figure 11.

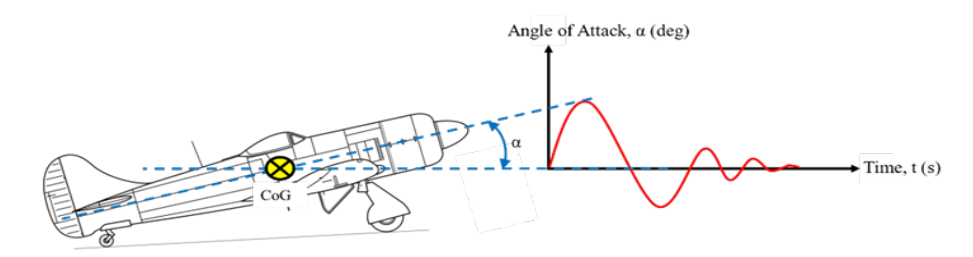


Figure 8. Short Period Mode for conventional aircraft. The oscillation occurs towards the angle-ofattack of the aircraft during flight

Phugoid Mode

This the second mode of the longitudinal mode for conventional aircraft. Phugoid mode represent the oscillatory motion of the aircraft canter of gravity during flight. This long period of oscillation will make the aircraft seem to go up and down event without any control surface been deflected. This oscillation is related to the aircraft speed during the occurrence of the motion. The phugoid mode is illustrated as in Figure 12.

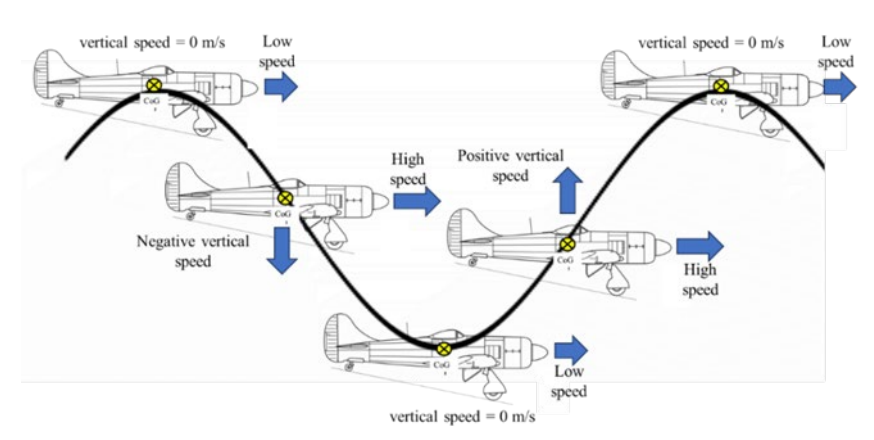


Figure 12. Phugoid Mode for conventional aircraft. The aircraft tend to move up and down during flight for a long period of time

The lateral and longitudinal modes mentioned above does not occur independently. Instead, all the mode occur conjunction with each other to form a complex behaviour or flight characteristic of the aircraft. However, for simplification, the lateral mode and the longitudinal mode are treated independently. This means that the Spiral Mode, Roll Mode, and Dutch Roll mode are grouped and studied together using the mathematical model in (2) while the Short Period Mode and Phugoid Mode are grouped and studied together using the mathematical model in (3). The flight modes discussed before can be tune accordance to pilot preference, passenger comforts and to meet the aviation authority requirements by implementing control laws using feedback approach that will enable engineer to alter the flight dynamics of the aircraft.

2.5 The Conventional Aircraft Attitude Control Laws Design

The attitude control laws (later known as control laws) designed for conventional aircraft are to tune the lateral and longitudinal mode of the aircraft flight characteristics to suit the design requirement of the aircraft manufacturer. Modern control laws for conventional aircraft utilized the pole placement method for MIMO system. This method allows for multiple outputs to be controlled based on available number of inputs by introducing a feedback gain between the outputs and inputs. The feedback gain for poles placement method is calculated from the desired poles sets by the control engineer designing the control laws for the conventional aircraft. The poles placement method alone is not enough to be used in the aircraft control laws. An open loop controller utilizing a pre-command gain needs to be added so that the inputs are equal to the desired outputs. This is crucial especially for the modern fly-by-wire conventional aircraft. The implementation of the pole placement method with open loop controller is as shown in Figure 13 for lateral flight and in Figure 14 for longitudinal flight.

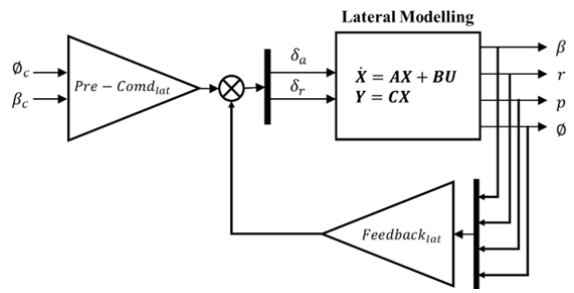


Figure 9. Lateral flight control laws for conventional aircraft

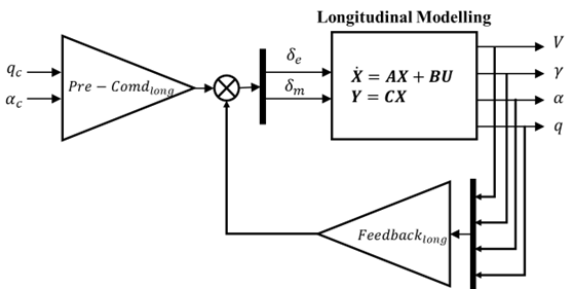


Figure 10. Longitudinal flight control laws for conventional aircraft

For lateral flight control laws in Figure 13, only bank angle and side slip angle can be controlled and for longitudinal flight control laws in Figure 14, only pitch rate and angle-of-attack can be controlled. This is due to the limitations of inputs available to control the outputs. Nonetheless, the control laws for lateral and longitudinal flight mentioned above are proven capable of handling the operation of conventional aircraft and is widely used in modern conventional aircraft.

2.6 The Conventional Aircraft and Conventional Fixed Wing Type UAV

In comparison, the conventional fixed wing type UAV or conventional UAV are relatively smaller compared to a conventional aircraft. This will limit the capacity of the UAV in term of numbers of sensors and flight computers that can be carry onboards. On a passenger aircraft, it can be more than 20 units of available sensors onboard the aircraft with more than five units of flight computers for data processing and control laws implementations. This is to ensure the overall safety and reliability through redundancy and segregation thus reducing the probability of system failure due to technical problems. Another important

aspect of conventional aircraft is the comfort of passengers and/or the cargo onboard the aircraft. As conventional aircraft are required to occasionally fly in moderately harsh environment, it is crucial that the passenger always feels comfortable. The control laws will always prioritize comfort second after safety as it is the main selling point to the industries.

For UAV on the other hand, passenger safety and comfort are not a priority. Most of the UAV available on the market are not designed to be flown in unordinary or harsh conditions. The range of flight is also shorter compared to conventional aircraft. This makes the UAV developed with a simpler design utilizing simpler hardware and sensors. However, having a conventional UAV with conventional aircraft capabilities will allow it to be flown in harsher conditions thus increase the UAV values in term of performance and capabilities. For the UAV to have the same capabilities as conventional aircraft, the readily available or readily designed UAV needs to be studied and compared with the conventional aircraft.

3.0 THE P15035 AIRCRAFT

The P15035 Aircraft is a UAV developed by The Aerobotics (Aerial Robotics) Research Group at Monash University [4]. This UAV is configured with a single motor and un-swept wings. The wings have a low aspect ratio with constant chord length [5]. There are only two control surfaces available which are a combination of ailerons and elevators which is called the elevons. The P15035 Aircraft is illustrated as in Figure 15.

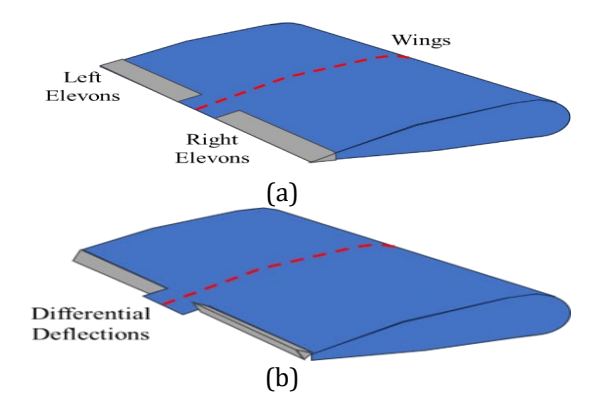


Figure 11. The P15035 Aircraft with single motor and elevons

In Figure 15, The P15035 Aircraft only has a pair of wings and a vertical tailplane. The wings are attached with elevons while the vertical tailplane has no control surfaces attached to it. This UAV have a single propeller for thrust generations.

3.1 The Inputs for P15035 Aircraft

The inputs for the P15035 Aircraft will be the elevons deflection specifically the left and right elevons deflections. When the elevons is deflected in the same direction, the elevons will be acting as an elevator. When the elevons are deflected in the different direction, it will act as ailerons [6]. This is illustrated as in Figure 16. From the illustration of elevons in Figure 16, the inputs for P15035 Aircraft are the elevons deflections specifically the left and right elevons deflections. This is as tabulated as in Table 5.



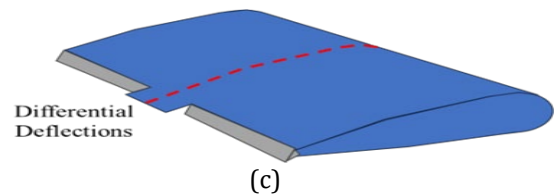


Figure 12. Elevons deflections on UAVs; (a) Elevons on wings, (b) Elevons act as ailerons, (c) Elevons act as elevator

Table 5. Inputs for P15035 Aircraft

1able 5. Inputs for 1 15055 / In craft	
Inputs	Symbols
Right Elevons Deflections	δ_R
Left Elevons Deflections	δ_L

The inputs in Table 5 are not ideal to be used for control design as both control surfaces need to be deflected at the same time to affect the UAV's attitude. The mixture of right elevons and left elevons deflection is a much preferable choices of inputs. Thus, the inputs for P15035 Aircraft are modified to be a mixture inputs as in Table 6. For P15035 Aircraft, the elevons are enough for it to control the lateral flight and longitudinal flight attitude.

Table 6. Mixtures inputs for P15035 Aircraft

1 0010 011111100	. 00 mp a 00 101 1 200	00 1111 01 01 0
Inputs	Symbols	Calculation
Summing of Inputs	$\delta_{\!\scriptscriptstyle A}$	$\delta_A = \delta_L + \delta_R$
Different of Inputs	δ_D	$\delta_D = \delta_L - \delta_R$

3.2 The Outputs for P15035 Aircraft

The outputs for P15035 depend on the flight controller used for the UAV. The flight controller used for this UAV is the MP2028g by MicroPilot. The MP2028g is equipped with 4 main sensors and a GPS for navigations [7]. The sensors are listed as Airspeed Sensor with the range from 0 kph up to 500 kph, Altimeter with the range from 0 m up to 12000 m, 3-Axes Angular Rate Gyroscope, Y-Axis accelerometer and GPS Module. The outputs for P15035 can be any kind of data processed from the sensors onboard the flight controller. However, for the modelling purposes, the outputs for the UAV are limited by the designer to only three as tabulated in Table 7. The outputs in Table 7 are used by the developer of the P15035 Aircraft to model the UAV inform mathematical equations.

Table 7. Outputs for P15035 Aircraft

Outputs	Symbols	Units	Remark
Roll Rate	р	rad/s	Lateral
Pitch Rate	q	rad/s	Longitudinal
Yaw Rate	r	rad/s	Lateral

3.3 The Modelling for P15035 Aircraft

The modelling for P15035 Aircraft is obtained by analysing the mathematical equations relating to the inputs in Table 6 and the outputs in Table 7. The data for the comparison is obtained through flight testing. The method of system identifications is used to obtain the mathematical modelling of this UAV with the result as in a mathematical equation in (4) [8].

$$\begin{pmatrix} p \\ q \\ r \end{pmatrix} = \begin{pmatrix} G_P & 0 \\ 0 & G_R \\ 0 & G_Y \end{pmatrix} \begin{pmatrix} \delta_A \\ \delta_D \end{pmatrix}$$
 (4)

where

$$G_P = \frac{-0.6503z(z + 0.0910)}{(z - 0.9115)(z^2 + 0.2267z + 0.3763)}$$

$$G_R = \frac{2.003z}{z^2 - 0.629z + 0.1441}$$

$$G_Y = \frac{-0.3688z(z - 8.25)}{(z - 0.9115)(z^2 - 0.629z + 0.1441)}$$

The modelling for P15035 Aircraft is different from the modelling of conventional aircraft. This is because the number of inputs and outputs used for modelling is far less than the conventional aircraft have.

3.4 P15035 Aircraft Flight modes

There is only one study on longitudinal flight mode and none on lateral flight mode for P15035 Aircraft. The flight mode studied are as in Table 8 and illustrated as in Figure 17 [9]. The longitudinal mode in Table 8 is obtained through observation of pitch rate output when the ailerons are acted as an elevator. Figure 17 shows that long period Phugoid mode has occurs during flight of the P15035 Aircraft. This result shows that flight modes can be observed even if there is only one output present.

Table 8. Longitudinal flight mode for P15035 Aircraft		
Flight Mode Characteristics		
Phugoid Mode	Overdamped & Large time constant	
Short Period Mode	Underdamped oscillation	

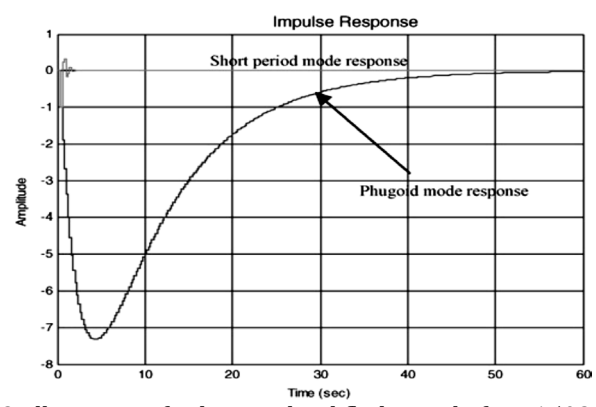


Figure 13. Illustration for longitudinal flight mode for P15035 Aircraft

3.5 Control Laws for P15035 Aircraft

There are two controller that has been tested for the P15035 Aircraft which are the PID controller and the H^{∞} controller. The designed controller however is only tested using simulation in MATLAB Simulink. The tested modelling in Simulink is illustrated as in Figure 18 for PID controller and in Figure 19 for H^{∞} controller [10].



Figure 18. Simulink diagram for PID controller for P15035 Aircraft

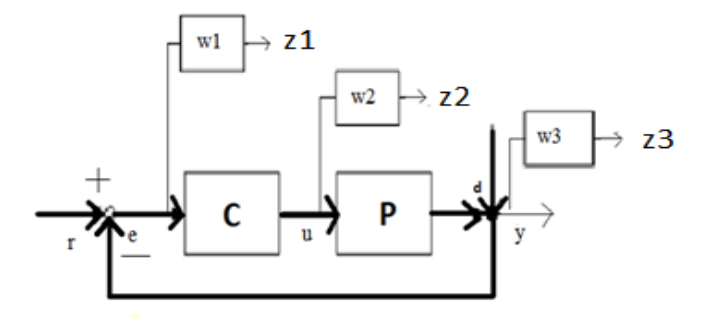


Figure 14. Simulink diagram for H∞ controller for P15035 Aircraft

The Simulink simulation results for PID controller in Figure 18 and $H\infty$ controller in Figure 19 shows significant improvements have been made by implementing the controller especially for the transient response time. The simulation result for the controller response compared to the natural response for P15053 Aircraft is as shown in Figure 20. The responses in Figure 20 shows that the implementation of PID controller and $H\infty$ controller will improve the performance of the UAV by shortening the response time reducing the effect of Phugoid flight mode.

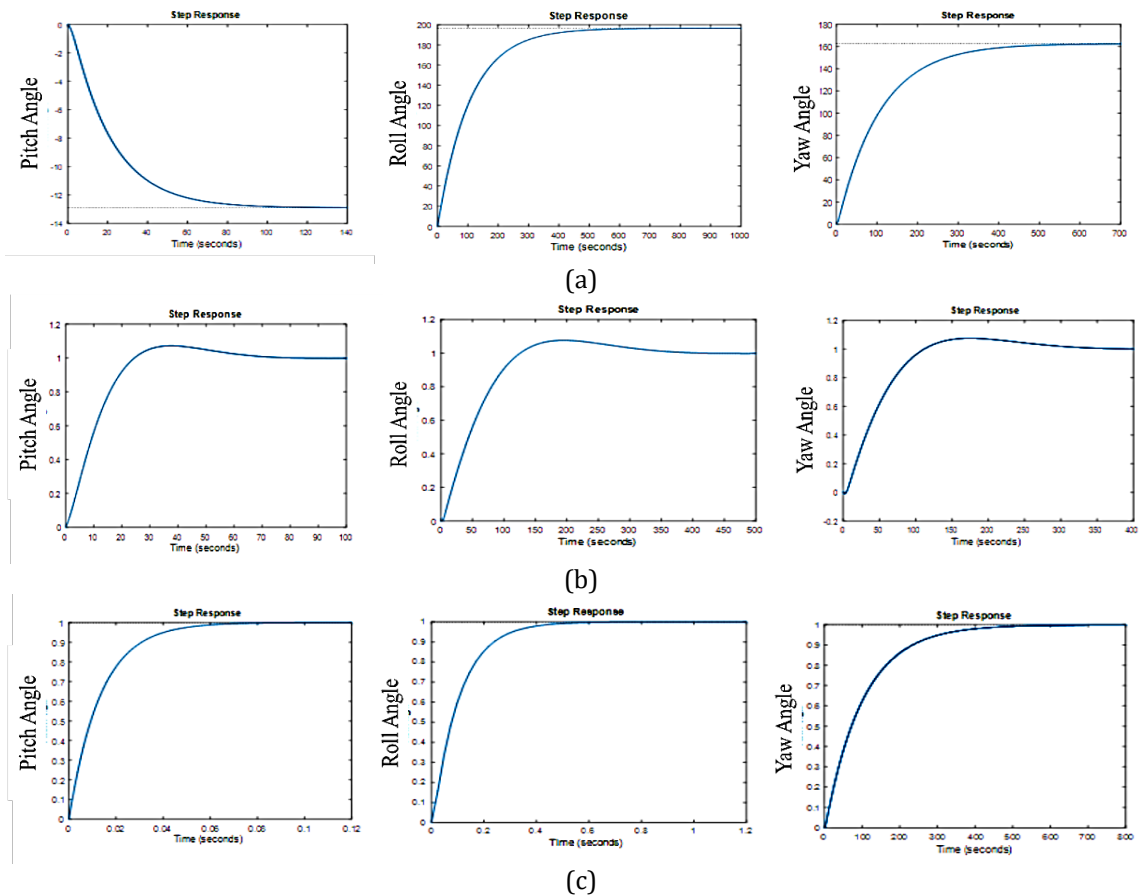


Figure 15. Comparison of responses for P15035 Aircraft [11]. Phugoid response has been reduced significantly; (a) Natural response of P15035 Aircraft, (b) Response of P15035 Aircraft with PID implementation, (c) Response of P15035 Aircraft with H∞ implementation

3.6 The P15035 Aircraft and Conventional Aircraft

Based on study conducted, the P15035 Aircraft is a small, fixed wing type UAV with two control surfaces for flight control. Conclusion can be made by comparing the P15035 Aircraft with conventional aircraft are as follows:

Sensors and Flight Controller

The P15035 Aircraft are using only values from the angular rate for modelling. This create a simple model yet proven to be sufficient for the small UAV. However, the flight controller used for this UAV is capable to provide extra sensors reading especially for airspeed which can allow better modelling to be done for the longitudinal modelling so for it to be identical to conventional aircraft modelling.

Flight Mode

The flight mode presented is only for longitudinal flight and it is a simplified mode utilising only the pitch rate reading. However, the flight mode has been successfully identified, and it shows that it is possible to determine the flight mode with only on sensor reading available.

Designed Controller

The results for the designed controller only show the responses simulated from the implemented controller design. Limitation such as maximum angle of deflection for elevons does not been considered while designing the controller. With the conclusion made above, the sensors, flight mode, and the designed controller need to be considered in advancing further into this whole project.

4.0 THE PEGASE

The PEGASE is a mini aerial vehicle (MAV) system that was designed and developed by École Nationale Supérieure D'Ingénieurs de Constructions Aéronautiques (ENSICA). This UAV is a delta wing type UAV with elevons as its control surfaces. This is a single motor UAV which can be flown up to speed of 20m/s. The PEGASE is as shown in Figure 21 with the general characteristic as Wingspan: 0.5m, Length: 0.34m, Wing Area: 0.0925m², Aerodynamic mean chord: 0.185m and Speed of cruising: 20m/s [12].



Figure 16. PEGASE mini-UAV

4.1 The Inputs for PEGASE

The input for PEGASE is the same as the P15035 Aircraft which utilized the elevons for manoeuvring during flight. Thus, the inputs for PEGASE are the same as in Table 6.

4.2 The Outputs for PEGASE

The developer of PEGASE has equipped this UAV with several functioning sensors including three units of Murata gyroscope to measure the angular rate of the UAV, two units of ADXL210 2-axes accelerometer for measuring accelerometer in 3 axes, temperature sensors to compensate for the temperature drift, honeywell three axes magnetic fields sensors for absolute reference for navigation and M-Blox GPS for position, altitude and speed measurement [13]. All the sensors mentioned above are connected to the Motorola 68332 microcontroller for computation. With all the sensors onboard, the PEGASE can produce 9 outputs that can be used for modelling. This is as tabulated in Table 9.

Table 9. Outputs for PEGASE			
Output	Symbol	Unit	
Velocity x-axis	V_{x}	m/s	
Velocity y-axis	$V_{\mathcal{Y}}$	m/s	
Velocity z-axis	V_z	m/s	
Pitch angle	heta	deg	
Heading angle	ψ	deg	
Roll angle	ϕ	deg	
Pitch Rate	q	deg/s	
Yaw Rate	r	deg/s	
Roll Rate	р	deg/s	

4.3 The Modelling for PEGASE

The modelling for PEGASE is done to find the mathematical equation representing the flight characteristics of PEGASE. This is done through wind tunnel testing in finding the relation between inputs in Table 6 and outputs in Table 9. The results of the modelling are as in (5) [14].

$$\dot{q} = -0.02V_x - 2.44V_z - 1.81\delta_A
\dot{\theta} = q
\dot{p} = -1.47\delta_D
\dot{\emptyset} = p$$
(5)

The model obtained in (5) is a linearized model from a complex mathematical modelling. The linearized model is simple yet obtains all the outputs from the sensors reading.

4.4 PEGASE Flight modes

The flight modes for PEGASE are not mentioned in any articles related to this UAV. Therefore, no explanation can be provided.

4.5 Control Law for PEGASE

The control laws for PEGASE are designed to control the UAV's attitude by manipulating four gains (k_{ij}) in the dynamic inversion equations in (6) [14].

$$\delta_A = -0.55k_{11}(k_{12}(\theta_d - \theta) - q)$$

$$\delta_D = -0.68k_{21}(k_{22}(\emptyset_d - \emptyset) - p)$$
(6)

The value for the four gains (k_{ij}) , can be obtain by solving the poles' location equations in (7).

$$P_{x} = \frac{-k_{i1} \pm \sqrt{k_{i1}^{2} - 4k_{i1}k_{i2}}}{2}, i = 1,2$$
(7)

With proper tools, the poles' location equation in (7) can be tune so that the flight characteristic for the PEGASE is accordance with the desired response as the engineering intended. The simulation for implementation of the feedback controller for PEGASE is as shown in Figure 22. The control laws method used in PEGASE is similar comparing to conventional aircraft as both are using the desire pole's location to calculate the feedback gain into the system. The method used for PEGASE is simpler and easier to implement into a microcontroller as it has been designed as such.

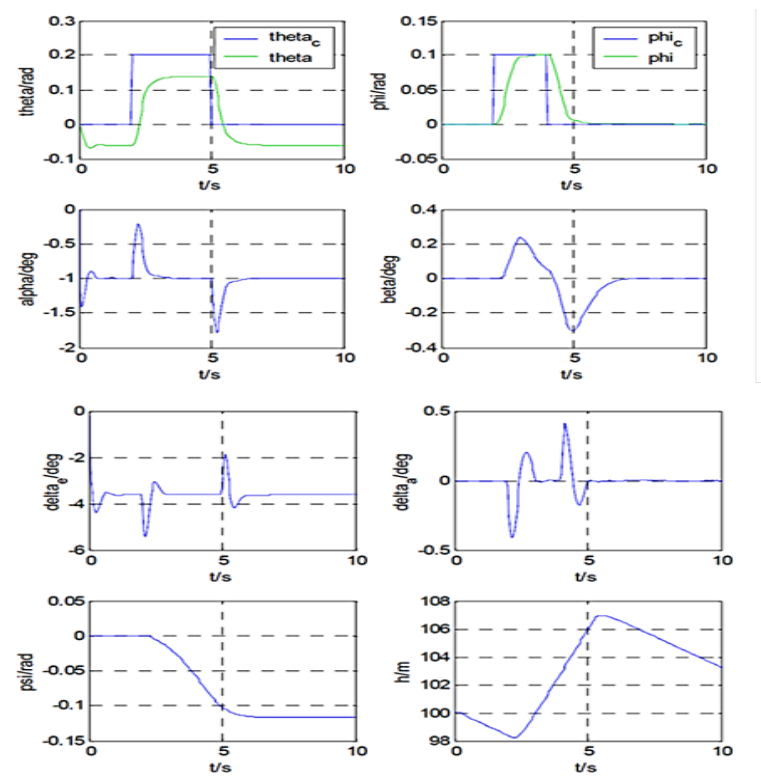


Figure 17. Example of simulation for feedback controller implementation for PEGASE [14]

4.6 The PEGASE and Conventional Aircraft

Compared to conventional aircraft, the PEGASE is relatively smaller in size. The design of body for PEGASE is also unconventional with delta wing configuration. From the literature study for PEGASE, the conclusion as follows can be made:

Inputs and Outputs

The inputs for PEGASE are still not enough for it to be similar with conventional aircraft. However, for the outputs, the 9 outputs present for this UAV make it much more comparable to the conventional aircraft. Only two drift-angles are still missing, which are the side slip angle and the angle of attack.

Sensor and Micro-controller

The PEGASE are not using an off-the-shelf flight controller. The flight controller is designed from scratch with a combination of microcontroller connected to sensors and peripherals. This approach allows the flight controller to be design custom for PEGASE UAV only. This resembles the conventional aircraft where every flight controller is different from one variant to the other.

Designed Controller

The designed controller for PEGASE is term of using the poles' location to determine the characteristics of the aircraft. However, the poles placement method used for the conventional aircraft is much more complex with more parameters to be tuned.

5.0 THE BPPT WULUNG

BPPT Wulung originally known as the LSU-05 is developed by Pusat Teknologi Penerbangan (Pustekbang) which is one of the aeronautical institutes in Indonesia. The BPPT Wulung is as shown in Figure 23 with basic characteristics as maximum take-off weight (MTOW) with 120kg, centre of gravity at 28% MAC, mean aerodynamic chord (MAC) at 0.6m, wing area is $3.717m^2$, horizontal tailplane area is $0.883m^2$, and Pitch moment inertia is $105.3kg.m^2$ [15].



Figure 18. BPPT Wulung

5.1 The Inputs for BPPT Wulung

The BPPT Wulung has the basic control surfaces to control the lateral and longitudinal flight of the UAV. The inputs for BPPT Wulung are tabulated as in Table 10. The inputs for BPPT Wulung in Table 10 are similar with conventional aircraft except for the lack of pitch trim deflection. This is because, for small UAV, the pitch trim deflection is unnecessary as the elevator can handle the longitudinal force during flight with the available control surface area.

Table 10. Inputs for BPPT Wulung

Inputs	Symbol	Remarks
Ailerons Deflection (rad)	δa	Lateral Motion
Rudder Deflection (rad)	δr	Lateral Motion
Elevator Deflection (rad)	δe	Longitudinal Motion

5.2 The Outputs for BPPT Wulung

Similar with the other two UAVs, the outputs for BPPT Wulung are depended on the sensors onboard the flight controller used to control the UAV flight. For BPPT Wulung, the flight controller used is the Pixhawk flight controller. The Pixhawk flight controller is a based on STM32 microcontroller which attached to multiple sensors as payload. It also can be used to attached external sensor through parallel connections.

For BPPT Wulung the sensors used are the internal Pixhawk sensors and GPS attached sensors. This sensor allows the BPPT Wulung to measure the outputs as in Table 11 to be used for modelling it.

Table 11. Outputs for BPPT Wulung

Outputs	Symbol	Unit
Airspeed	v	m/s
Yaw Rate	r	rad/s
Roll Rate	p	rad/s
Bank Angle	Ø	rad
Axial Velocity	и	m/s
Normal Velocity	w	m/s
Pitch Rate	q	rad/s
Pitch Angle	heta	rad

5.3 The Modelling for BPPT Wulung

The modelling for BPPT Wulung is done for the longitudinal flight dynamics of the UAV. There are three methods been tested for modelling this UAV which are as follows [16]:

Analytical Method

The analytical method is done by calculating the aerodynamics coefficient for the BPPT Wulung using a specific computational aided software (DATCOM). The aerodynamic coefficients are calculated by the utilising the finite element methods onto the UAV 3D model. The model resulted from this method is a state-space representation as shown in (8).

$$\begin{pmatrix} \dot{u} \\ \dot{w} \\ q \\ \dot{\theta} \end{pmatrix} = \begin{pmatrix} -0.0349 & 0.2544 & 0 & -9.81 \\ -0.5155 & -3.9952 & 35.0005 & 0 \\ 0.9295 & 6.1888 & -68.0346 & 0 \\ 0 & 0 & 1 & 0 \end{pmatrix} \cdot \begin{pmatrix} u \\ w \\ q \\ \theta \end{pmatrix} + \begin{pmatrix} -0.6168 \\ -5.4665 \\ -6.0996 \\ 0 \end{pmatrix} \cdot \delta_e$$

$$Y = \begin{pmatrix} 1 & 0 & 0 & 0 \\ 0 & 1 & 0 & 0 \\ 0 & 0 & 1 & 0 \\ 0 & 0 & 0 & 1 \end{pmatrix} \cdot \begin{pmatrix} u \\ w \\ q \\ \theta \end{pmatrix}$$

$$(8)$$

Empirical Black Box Method

This method is done using system identification process to determine the valid mathematical model representing the BPPT Wulung UAV. This is done by determine the best mathematical equations that fit the relations between the inputs and the outputs of the UAV. The inputs and outputs data are collected through flight testing and MATLAB system identification toolbox is used to do the system identification process. The modelling produce from the Black Box method is a state-space representation as in (9) with the comparison with real data as in Figure 24.

$$\begin{pmatrix} \dot{u} \\ \dot{w} \\ \dot{q} \end{pmatrix} = \begin{pmatrix} -0.2183 & -0.2247 & 4.9895 & -9.1839 \\ -0.1367 & -0.2327 & 10.5920 & -2.9838 \\ 0.0085 & -0.0702 & -3.2819 & -0.5656 \\ -0.0001 & -0.0016 & 0.9687 & -0.0137 \end{pmatrix} \cdot \begin{pmatrix} u \\ w \\ q \\ \theta \end{pmatrix} + \begin{pmatrix} 1.7542 \\ 2.3014 \\ -4.7408 \\ -0.0629 \end{pmatrix} \cdot \delta_e$$

$$Y = \begin{pmatrix} 1 & 0 & 0 & 0 \\ 0 & 1 & 0 & 0 \\ 0 & 0 & 1 & 0 \\ 0 & 0 & 0 & 1 \end{pmatrix} \cdot \begin{pmatrix} u \\ w \\ q \\ \theta \end{pmatrix}$$

$$(9)$$

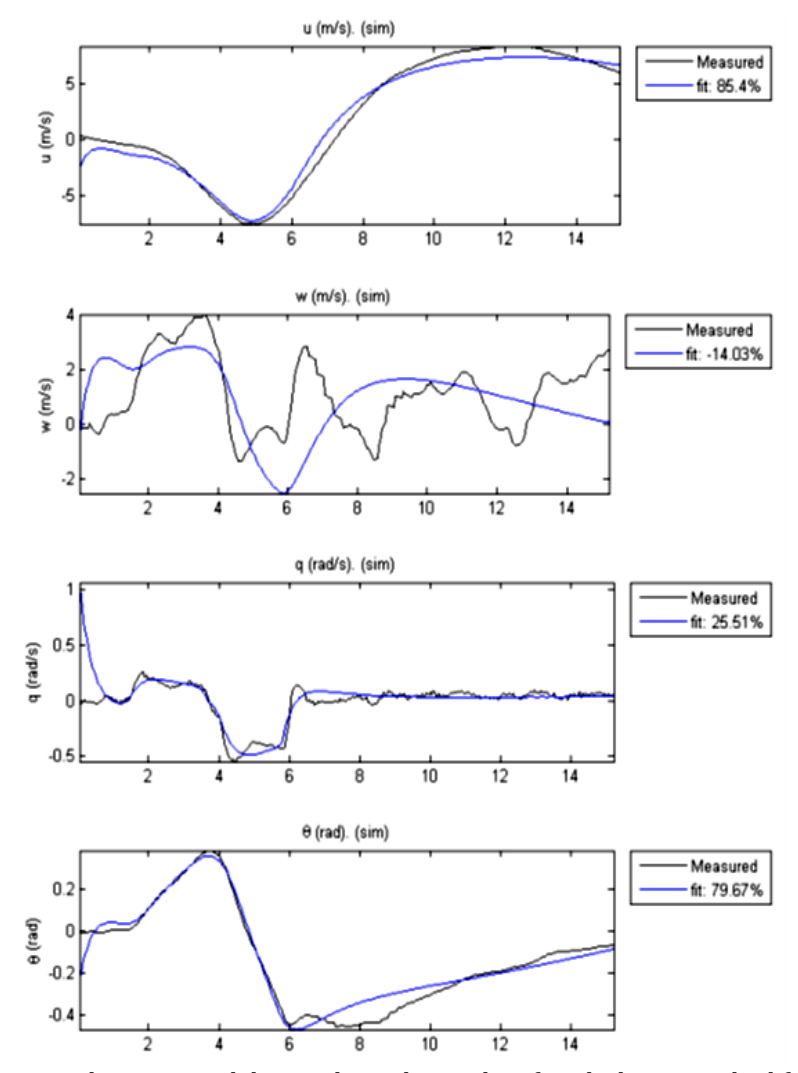


Figure 19. Comparison between real data and simulation data for Black Box method for BPPT Wulung

Empirical Grey Box Method

Grey Box method utilised the relation between inputs and outputs to build a mathematical modelling just like a Black Box method does. Additional to the Black Box method, the Grey Box method uses the physical principles from the analytical model with a Kalman Filter applied to reduce measurement noises to build a new mathematical modelling representing the UAV. This method allows the fitting to be significantly improve compared to Black Box method. The results from the Grey Box are a state-space modelling in (10) with comparison with real data as in Figure 25.

$$\begin{pmatrix}
\dot{u} \\
\dot{w} \\
q \\
\dot{\theta}
\end{pmatrix} = \begin{pmatrix}
194.27 & 1311.1 & -14232.7 & -9.81 \\
-3321.9 & -22408.0 & 242997.2 & 0 \\
117.63 & 793.25 & -8607.7 & 0 \\
0 & 0 & 1 & 0
\end{pmatrix} \cdot \begin{pmatrix} u \\ w \\ q \\ \theta \end{pmatrix} + \begin{pmatrix} -1098.8 \\ 18427.7 \\ -659.26 \\ 0 \end{pmatrix} \cdot \delta_e$$

$$Y = \begin{pmatrix}
1 & 0 & 0 & 0 \\
0 & 1 & 0 & 0 \\
0 & 0 & 1 & 0 \\
0 & 0 & 0 & 1
\end{pmatrix} \cdot \begin{pmatrix} u \\ w \\ q \\ \theta \end{pmatrix} \tag{10}$$

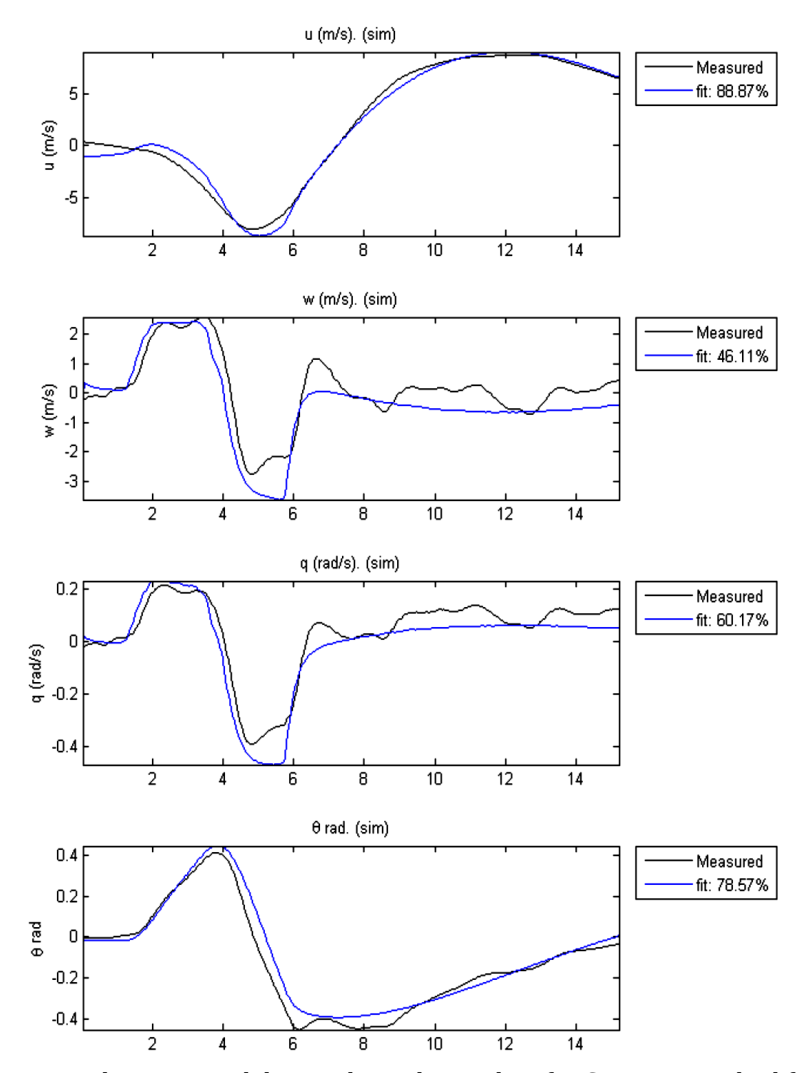


Figure 20. Comparison between real data and simulation data for Grey Box method for BPPT Wulung

Comparing the results for Black Box method in Figure 24 and the results from the Grey Box method in Figure 25, it is shown that the Grey Box method is superior in term of fitting percentages thus provide a better modelling for the UAV.

5.4 The BPPT Wulung Flight Modes

The are no studies done for flight modes and control laws development for BPPT Wulung. Therefore, there are no results can be compared for the flight modes and control laws design. However, the studies on BPPT Wulung modelling are valuable for this project as it provides an insight on how a complex modelling can be done for a small fixed-wing type UAV.

5.5 The BPPT Wulung and Conventional Aircraft.

The studied of BPPT Wulung indicate that there is only longitudinal modelling was done this UAV. Comparing to conventional aircraft, several conclusions can be made as follows:

Modelling

The Grey Box modelling method is the best method to obtain the state-space representation model which is a similar representation used in conventional aircraft. However, this method requires for analytical model of the UAV to be obtained first before it can be in cooperated with the flight test data. This indicate that there is high level of complexity for utilising this method.

Inputs

The modelling for BPPT Wulung using Grey Box method is indeed very impressing. However, the model produce is still not similar to the conventional aircraft modelling. This is due to the absent of pitch trimming input for the UAV.

6.0 FINDING ON LITERATURE REVIEW

The findings for literature review are categorised into two categories. The first categories will be the general findings on comparison between conventional aircraft and available developed UAV available. The second categories will be the findings related to developing the chosen UAV for this project (FT Guinea Pig) for it to be able to be modelled similar as conventional aircraft and to enable for control laws to be designed for it

6.1 General Finding

Several findings comparing the conventional aircraft with the studied UAV can be observed as follows:

Inputs

The inputs for UAV are smaller in number compared to the conventional aircraft. The minimum number of control surfaces on a fixed wing UAV must be at least two (elevons) while some of UAV utilised three control surfaces (ailerons, rudder, elevator) for inputs. The pitch trim control surfaces are not applied on fixed wing UAV because it will increase weight at the tail sections of the UAV and upset the centre of gravity.

Outputs

Most of the outputs for UAVs are depended on the onboard sensors on a flight controller. Some flight controllers have limited number of onboard sensors thus reduce the number of outputs to be generated. For Pixhawk flight controller for examples, external sensors can be attached to increase the number of outputs available thus allow for more outputs to be generated. Nonetheless, the main outputs for any UAV will be attitude measurements of the UAV (Roll, Pitch, Yaw). The custom developed flight controller is superior in term of customisable numbers of onboard sensors. The custom developed flight controller can also be specifically designed for a specific UAV thus reduce the number of unnecessary sensors that never going to be used for the UAV.

Control Laws Design

The control laws designed for conventional aircraft requires complex and tedious process. Most UAV utilised a simple control laws schemes as it is easier to be implemented and there is no restriction for payload comfort. For similar control laws in conventional aircraft to be implemented onto a UAV, the model needed to be similar first.

6.2 Finding for Future Project Development

The findings for project development are focusing on how to utilise the chosen UAV for it to have similar inputs and outputs so that the modelling and control laws can be designed like the conventional aircraft. The finding for this is as follows:

Inputs

For a UAV to be modelled comparable with conventional aircraft, the basic inputs of ailerons, rudder and elevator are necessary. The pitch trim deflection is not necessary as the UAV will be small in sized which make the pitch trim ineffective.

Outputs

The outputs for modelling the UAV comparable with conventional aircraft will be the side-slip angle, yaw rate, roll rate, bank angle, angle-of-attack, pitch rate, and pitch angle. The flight path angle may be replaced

by the pitch angle for simplicity. The attitude angle measurement (yaw rate, roll rate, bank angle, pitch rate, and pitch angle) may be calculated using sensors fusion using IMU utilising Kalman filtering as demonstrated Liu et al. as shown in Figure 26. The drift angle measurement (side-slip angle and angle-of-attack) may be obtained using differential pressure calculations or vane effect sensor as shown in Figure 27 and Figure 28 respectively.

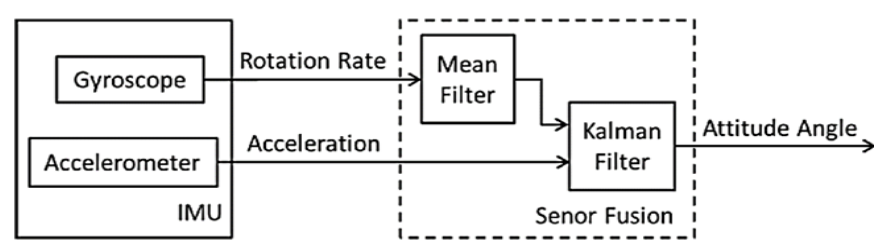


Figure 21. IMU implementation for attitude measurement [17]

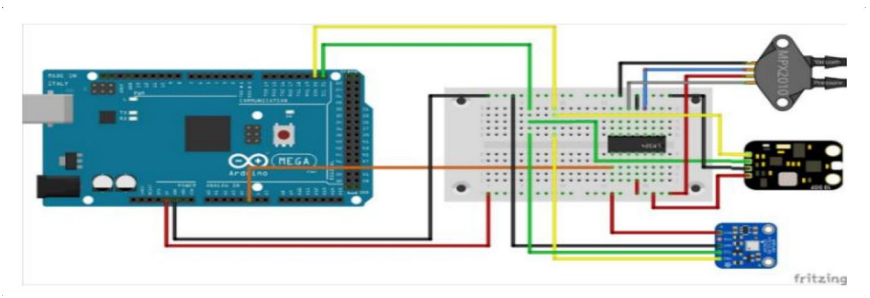


Figure 22. Drift angle sensor [18]

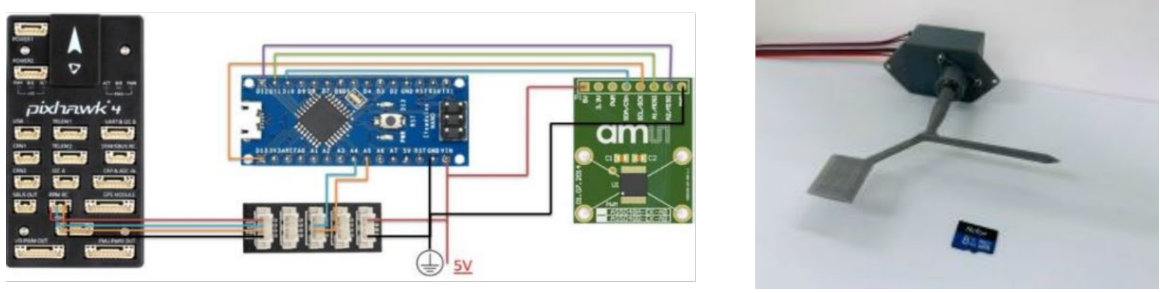


Figure 23. Angle-of-attack sensor [19]

Modelling

The best way for modelling the UAV comparable with conventional aircraft will be using the Grey Box method demonstrated in BPTT Wulung Modelling. However, the Black Box method will be the easiest as it only required the flight-testing data for modelling.

Control Laws Design

The suitable control laws design for modelling the UAV comparable with conventional aircraft is a poles placement method. Consideration for the poles' placement method are for 2 inputs and 4 outputs systems, the feedback gain will in the form of 2 by 4 matrix, two feedback gain can be obtained that can produce two difference responses but having the same characteristics, state coupling and decoupling can be used to improve the outputs response and the pre-command gain can be used to coupling the inputs with desired outputs and eliminate the steady state error [20].

7.0 CONCLUSIONS

In conclusion, the literature review has been successfully conducted by comparing the conventional aircraft with three available UAV. It can be concluded that for modelling the UAV comparable with conventional aircraft attitude measurement using IMUs and drift angle measurement/calculation need to be done before modelling process and control laws can be designed and implemented.

8.0 CONFLICT OF INTEREST

The authors declare no conflicts of interest.

9.0 AUTHORS' CONTRIBUTION

Abdul Rashid, Z. (Methodology; Validation; Formal analysis; Investigation; Writing -original draft) Syed Mohd Dardin, S. M. F. (Formal analysis; Investigation) Ahmad, K. A. (Supervision; Project administration)

10.0 ACKNOWLEDGEMENTS

This study was not supported by any grants from funding bodies in the public, private, or non-profit sectors. The authors fully acknowledged Ministry of Higher Education (MOHE) and National Defence University of Malaysia (NDUM) which makes this important research viable and effective.

List of Reference

- [1] PRIME Faraday Partnership (2002). An Introduction to MEMS, United Kingdom: Loughborough University.
- [2] Aragao, P. (2012) Photo of F-WWIQ Airbus A320-216 Aibus Industrie," JETPHOTOS.NET, Toulouse.
- [3] AIRBUS S. A. S. (2020), A320 Aircraft Characteristics Airport and Maintainance Planning, Blagnac Cedex: AIRBUS S. A. S.
- [4] Barba, M. (2015). Autoflight, Toulouse: AIRBUS OPERATION SAS.
- [5] The Centre for Telecommunications and Information Engineering (CTIE), "CTIE Aerobotics U A V Research Group," Monash Universiti, 21 October 2007. [Online]. Available: https://www.ctie.monash.edu.au/AEROBOTICS/. [Accessed 31 January 2021].
- [6] Aerobotics@Monash, "Aerobotics Archive," Aerobotics, 30 November 2007. [Online]. Available: https://www.eganfamily.id.au/archive30nov2007/monash/research/uav/aerobotics/aerobotics_aircraft.html#p16025andp15035. [Accessed 31 January 2021].
- [7] Kundu, A. K., Price, M. A., & Riordan, D. (2019). *Conceptual aircraft design: an industrial approach*. John Wiley & Sons.
- [8] MicroPilot (2010). MP2x28 Family of Uav Autopilots, MicroPilot, Manitoba.
- [9] Liu, M., Egan, G., & Ge, Y. (2006, October). Identification of attitude flight dynamics for an unconventional UAV. In 2006 IEEE/RSJ International Conference on Intelligent Robots and Systems (pp. 3243-3248). IEEE.
- [10] Santoso, F., Liu, M., & Egan, G. (2008). H 2 and H∞ robust autopilot synthesis for longitudinal flight of a special unmanned aerial vehicle: a comparative study. *IET Control Theory & Applications*, *2*(7), 583-594.
- [11] Liu, M., Egan, G. K., & Santoso, F. (2015). Modeling, autopilot design, and field tuning of a UAV with minimum control surfaces. *IEEE Transactions on Control Systems Technology*, *23*(6), 2353-2360.
- [12] Parra, C., Su, B., Bordeneuve Guibe, J., & Briere, Y. (2003). Modelisation and Instrumentation of a Mini UAV: PEGASE," Journees Doctoral d'Automatique.
- [13] Parra, C., Su, B., Bordeneuve Guibe, J., & Briere, Y. (2002). Development of a MAV—from theory to implementation. In *EURO-AUVSI Conference*.
- [14] Briere, Y., Parra, C., Guibe, J. B., & Sola, J. (2003). A mini aerial vehicle as a support for modelling, control and estimation teaching. *IFAC Proceedings Volumes*, *36*(10), 273-278.
- [15] Triputra, F. R., Trilaksono, B. R., Adiono, T., Sasongko, R. A., & Dahsyat, M. (2015). Nonlinear dynamic modeling of a fixed-wing unmanned aerial vehicle: A case study of Wulung. *Journal of Mechatronics, Electrical Power, and Vehicular Technology, 6*(1), 19-30.
- [16] Triputra, F. R., Trilaksono, B. R., Sasongko, R. A., & Dahsyat, M. (2012, September). Longitudinal dynamic system modeling of a fixed-wing UAV towards autonomous flight control system development: A case study of BPPT wulung UAV platform. In 2012 International Conference on System Engineering and Technology (ICSET) (pp. 1-6). IEEE.
- [17] Liu, Y., Noguchi, N., & Ishii, K. (2014). Development of a low-cost IMU by using sensor fusion for attitude angle estimation. *IFAC Proceedings Volumes*, *47*(3), 4435-4440.

- [18] Ariante, G., Ponte, S., Papa, U., & Del Core, G. (2021). Estimation of airspeed, angle of attack, and sideslip for small unmanned aerial vehicles (UAVs) using a micro-pitot tube. *Electronics*, 10(19), 2325.
- [19] Wanngoen, K., Saetunand, N., Saengphet, W., & Tantrairatn, S. (2020, January). Angle of attack sensor for small fixed-wing unmanned aerial vehicles. In *Proceedings* (Vol. 39, No. 1, p. 19). MDPI.
- [20] Rashid, Z. A., Dardin, S. M. F. S. M., Ahmad, K. A., & Azid, A. A. (2025). Modelling and implementation of control law design for UAV control surface using PIDs controller and feedback controller with integrator. *Zulfaqar Journal of Defence Science, Engineering & Technology, 8*(1).